

## The Conformations and Vibrational Spectra Including Matrix Isolation of 1,3-Dibromo-2,2-dimethylpropane

A. Gatial\*, P. Klæboe, C. J. Nielsen, and D. L. Powell\*\*

Department of Chemistry, University of Oslo, 0315 Oslo 3, Norway

Received November 19, 1987

The IR spectra of 1,3-Dibromo-2,2-dimethylpropane as a liquid and as two crystalline solids obtained at low temperature and at high pressure were recorded. Additional IR spectra of this compound, matrix isolated in argon and nitrogen at 14 K, were obtained using nozzle temperatures of 300, 450 and 700 K. Raman spectra including polarization measurements were recorded at various temperatures between 340 and 230 K. Crystalline solids were obtained by freezing the liquid and by shock freezing the vapour at 85 K with subsequent annealing.

The GG and AG conformers were present in the low temperature and in the high pressure crystals, respectively, and the enthalpy differences were 5.6 (liquid) and 4.2 kJ mol<sup>-1</sup> (vapour) with GG being the more stable. An additional conformer AA was detected in the liquid and in the matrix isolated spectra, being approximately 6.4 and 6.5 kJ mol<sup>-1</sup> less stable than GG in the liquid and vapour, respectively. Vibrational assignments of the GG and AG spectra are presented, supported by a normal coordinate analysis.

### INTRODUCTION

Neopentane (C(CH<sub>3</sub>)<sub>4</sub>) has a spherical shape and represents an interesting derivative of propane. If at least two hydrogens attached to different carbon atoms are substituted with halogens, the molecules will have conformers of different abundance.<sup>1</sup> Neopentane<sup>2</sup> and some<sup>3</sup> of the halogenated derivatives have plastic phases, stable in the temperature range between the low temperature anisotropic crystal phase and the liquid, while other neopentanes have no plastic phases.<sup>4</sup>

The vibrational spectra of various halogenated neopentanes have recently been investigated in our laboratory, including 1-chloro-2,2-dimethylpropane,<sup>5</sup> 1,3-dichloro-2,2-dimethylpropane (DCDMP),<sup>6</sup> 2-(chloromethyl)-2-methyl-1,3-dichloropropane<sup>7</sup> and 2,2-di(chloromethyl)-1,3-dichloropropane<sup>8</sup> and 2,2-di(bromomethyl)-1,3-dibromopropane.<sup>8</sup> Apart from the latter two compounds, all of these exhibited plastic phases. Due to the interesting conformational properties of these molecules we decided to extend our studies to include 1,3-di-

\* On leave from Department of Physical Chemistry, Slovak Technical University, 81237 Bratislava, Czechoslovakia, ČSSR.

\*\* On leave from the College of Wooster, Wooster, OH 44691, U.S.A.

bromo-2,2-dimethylpropane (hereafter abbreviated DBDMP); certain preliminary observations have recently been published.<sup>9</sup> A full account of our results for DBDMP, including conformational stabilities, the conformation present in the crystal phases and complete interpretations of the spectra are given in the present paper.

#### EXPERIMENTAL

DBDMP was purchased from ICN Pharmaceuticals Inc. and purified by preparative gas chromatography. Its identity was confirmed by mass spectroscopy. IR spectra of the low temperature amorphous and annealed crystalline solids deposited on a CsI window ( $4000\text{--}200\text{ cm}^{-1}$ ) at 85 K were obtained. The sample was isolated in argon and nitrogen matrices (1:500), deposited at 14 K from vapour mixtures at 300, 450 and 700 K by means of an electrically heated quartz nozzle. High pressure spectra were obtained with a diamond anvil cell (DAC) with diamonds of type IIa, equipped with a spacer of bronze and interfaced with a 4x beam condensor from P.-E. The sample was carefully observed in a polarization microscope during the increase and decrease of the pressure.

The IR spectra were recorded with a Perkin-Elmer model 225 spectrometer ( $4000\text{--}200\text{ cm}^{-1}$ ) and an evacuable FTIR model 114c from Bruker ( $4000\text{--}40\text{ cm}^{-1}$ ). A closed cycle helium cooled cryostat from Air Products was employed for the matrix isolation experiments.

The Raman spectra were recorded with a Dilor triple monochromator spectrometer RT 35 interfaced with the Aspect 2000 computer of the Bruker spectrometer. A Spectra Physics argon ion laser model 2000 was employed using the 514.5 nm line with  $90^\circ$  and  $180^\circ$  illumination geometries. Low temperature Raman spectra of the liquid and of the crystalline solid were obtained in a glass tube of 2 mm inner diameter surrounded by a Dewar cooled by gaseous nitrogen.<sup>10</sup> Conventional cryostats cooled with liquid nitrogen consisting of either a cooled copper finger (Raman) or a CsI (mid IR) or Si window (far IR) were employed for the amorphous and crystalline solids.

#### RESULTS

Among the large number of the recorded spectra, we have reproduced IR spectra of the amorphous and crystalline solids at 85 K in the regions  $1500\text{--}1200\text{ cm}^{-1}$  (Figure 1) and  $1000\text{--}400\text{ cm}^{-1}$  (Figure 2). An IR spectrum of a high pressure crystal is reproduced in Figure 3, whereas those of DBDMP matrix isolated in nitrogen with nozzle temperatures of 300 and 700 K are given in Figure 4. Parts of the Raman spectra of DBDMP as a liquid and

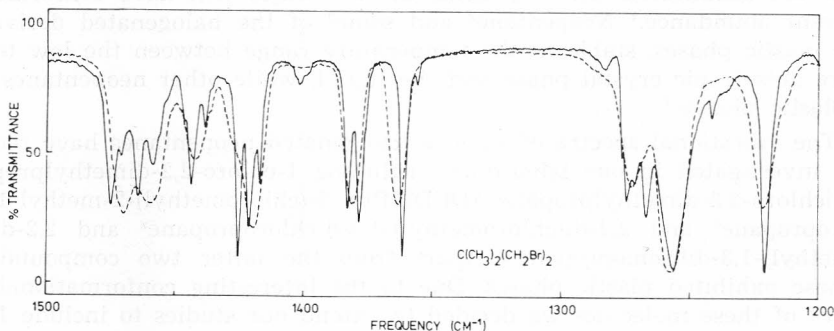


Figure 1. IR spectrum of 1,3-Dibromo-2,2-dimethylpropane (DBDMP) in the  $1500\text{--}1200\text{ cm}^{-1}$  range as an amorphous (dotted line) and annealed crystalline sample (solid line) at 85 K.

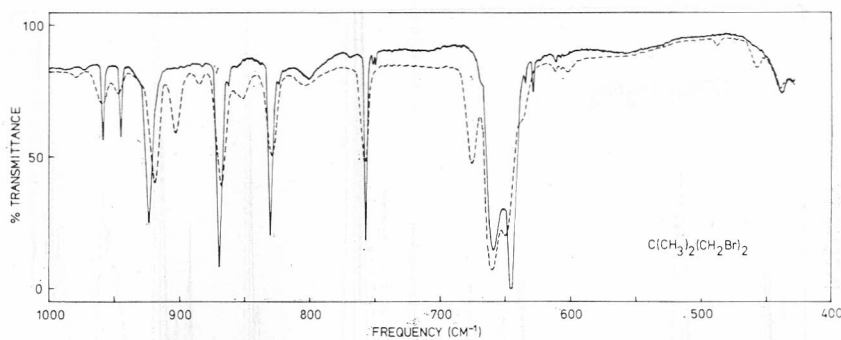


Figure 2. IR spectrum of DBDMP in the 1000–400  $\text{cm}^{-1}$  range as an amorphous (dotted line) and annealed crystalline sample (solid line) at 85 K.

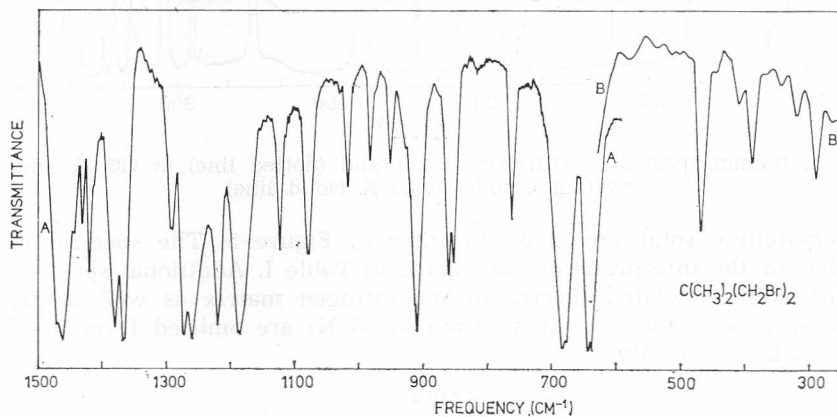


Figure 3. IR spectra of DBDMP as a high pressure crystal at ca. 20 kbar, curve A, resolution 2  $\text{cm}^{-1}$ , curve B resolution 8  $\text{cm}^{-1}$ .

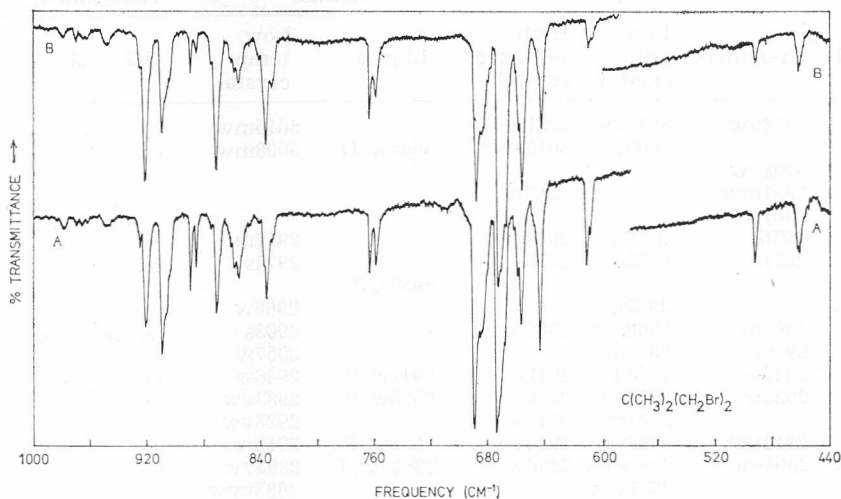


Figure 4. IR spectra of DBDMP in nitrogen matrices (1:500) recorded at 14 K, nozzle temperatures 700 K (curve A) and 300 K (curve B) in the range 1000–400  $\text{cm}^{-1}$ .

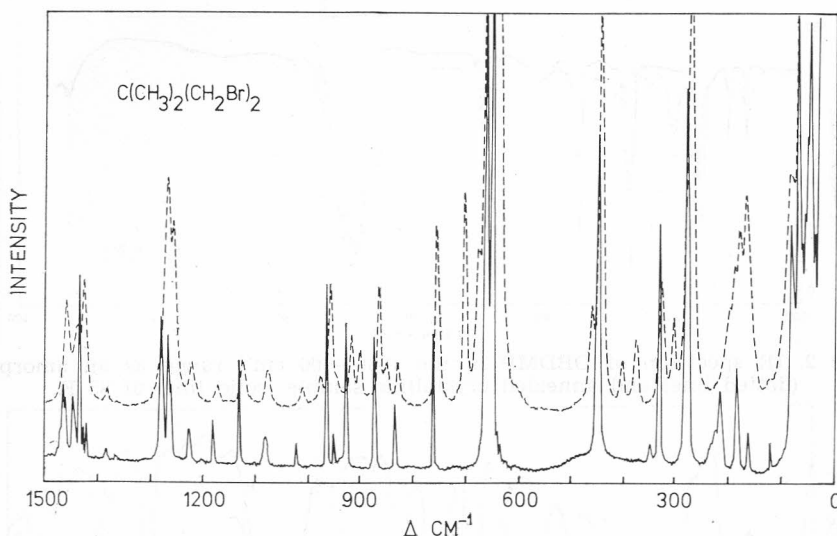


Figure 5. Raman spectra of DBDMP as a liquid (dotted line) at 285 K and as a crystalline solid at 85 K (solid line).

as a crystalline solid are given together in Figure 5. The spectral results essential for the interpretations are listed in Table I. Additional spectral data (e. g. IR matrix isolated spectra in the nitrogen matrix as well as IR and Raman spectra of the amorphous solid at 85 K) are omitted from the Table for the sake of brevity.

TABLE I

*Infrared and Raman Spectral Data for 1,3-Dibromo-2,2-Dimethylpropane (DBDMP)<sup>a</sup>*

Infrared				Raman		Assignment <sup>b</sup>			
Liquid	Ar-matrix	Low. temp. crystal	High pressure crystal	Liquid	Low temp. crystal	GG	AG	AA	
3006w	3018vw <sup>c</sup>	3015vw	3031mw	3008w, D	3015mw	$\nu_1$	$\nu_1$		
		3009vw	3019mw		3008mw	$\nu_{24}$	$\nu_2$		
	3002vw								
	2991mw		2988m						
	2981w								
2966s	2976s	2977m	2984s	2959s, P	2977m	$\nu_2$	$\nu_3$		
	2971s	2973s	2978s		2974s	$\nu_{25}$	$\nu_4$		
		2965w			2966w				
	2964m	2962s	2966mw		2963s	$\nu_3, \nu_{26}$	$\nu_5, \nu_6$		
2941w	2959vw	2956m			2957w				
	2947w	2948w	2941s	2942w, P	2946w	$\nu_4$	$\nu_7$		
2931w	2935w	2933vw	2928vw	2928w, P	2933vw	$\nu_{27}$	$\nu_8$		
		2921vw	2918w		2923vw				
2908w	2912vw	2907vw	2913vw	2908w, P	2910w				
2894vw	2894vw	2892vww	2896w	2893vw, P	2893vw	$\nu_5$	$\nu_9$		
		2881vww			2883vww				
		2874vw							

Table I cont'd.

Infrared				Raman		Assignment <sup>b</sup>		
Liquid	Ar-matrix	Low. temp. crystal	High pressure crystal	Liquid	Low temp. crystal	GG	AG	AA
2872w	2875vw	2871w	2877w	2878vw, P	2872w	$\nu_{28}$	$\nu_{10}$	
		2859w			2860w			
	2847vw	2850w			2850w			
2837w	1473s	2838w	2835w	2835w	2837vvw	$\nu_{29}$		
		1475s			1472vvw			
		1471w						
1470s	1467m $\uparrow$		1471s					$\nu_{11}$
1463m	1464w	1465s	1461s		1464m	$\nu_6$	$\nu_{12}$	
				1460s, P				
1460w	1459w	1459w	1456w		1459w	$\nu_{30}$	$\nu_{13}$	
1443w	1444w	1444m	1446w	1441m, P	1445m	$\nu_7$	$\nu_{14}$	
1428w	1428m	1426vs	1431m		1433s	$\nu_8$	$\nu_{15}$	
				1428s, P				
		1422s			1426w			
1423s	1425s	1418m	1420s		1420w	$\nu_{31}$	$\nu_{16}$	
	1386s	1383s						
1384s	1384w	1379s	1380s	1385vw, P	1382vvw	$\nu_9$	$\nu_{17}$	
	1372vw							
	1369m $\uparrow$	*	1367s				$\nu_{18}$	
1366s	1367s	1362vs	*	1367vvw	1365vvw	$\nu_{32}$		
	1362vvw							
	1289vw $\uparrow$	*	1291m				$\nu_{19}$	
1286w	1278mw	1275m	*	1287vvw	1278s	$\nu_{33}$		
	1271vw $\uparrow$	*	1275s				$\nu_{20}$	
1270m	1267m	1267s	*	1269vs, P	1263s	$\nu_{10}$		
	1262vs	1256vs	*		1259m	$\nu_{34}$		
1257vs	1257m $\uparrow$	*	1260s	1258m, D				$\nu_{21}$
	1231m							
1223s	1225m	1221vs	*	1222w, P	1224w	$\nu_{11}$		
1214m	1215w $\uparrow$	*	1220s	1215vw, P $\uparrow$	*		$\nu_{22}$	
	1213vw							$\nu_{23}$
	1183mw	$\uparrow$ *	1185s					
1180m	1181mw							
	1178m							
1172s	1176m	1176m	*	1173w, D	1177mw	$\nu_{35}$		
1153w	1155vw $\uparrow$	*	*					AA
1126s	1128w	1126s	*	1126w, P?	1127m	$\nu_{12}$		
1120w	1119vw $\uparrow$	*	1123m	1119vw $\uparrow$	*		$\nu_{24}$	
	1089vw	1079w						
1079m	1083w	1076m		1077w, D	1078w	$\nu_{36}$		
	1077vw	$\uparrow$ *	1079m				$\nu_{25}$	
1076m	1073vw							

Table I cont'd.

Infrared				Raman		Assignment <sup>h</sup>		
Liquid	Ar-matrix	Low. temp. crystal	High pressure crystal	Liquid	Low temp. crystal	GG	AG	AA
1012w	1011w	1016m	} 1018mw	1011w, P	1017w	$\nu_{13}$	$\nu_{26}$	
		1013m						
977w	978vw $\uparrow$	*	983mw	976w, P $\uparrow$	*		$\nu_{27}$	
958mw	960vw	959m	*	958m, P	960m	$\nu_{14}$		
947w	946vw	946m	951mw	947vw, D	947w	$\nu_{37}$	$\nu_{28}$	
917s	921s	924s	*	918mw, D	924m	$\nu_{38}$		
901s	904m $\uparrow$	*	910s	902w, P? $\uparrow$	*		$\nu_{29}$	
884w	888w $\uparrow$	*	*	886vw	*			AA
866s	872m	870vs	*	866m, P	870m	$\nu_{15}$		
850s	855mw $\uparrow$	*	861m	851w, P $\uparrow$	*		$\nu_{30}$	
	838w	} 830s	853m	830w, D	830mw	$\nu_{39}$	$\nu_{31}$	
830s	833m							
	768vw	} 757s	763m	757m, P	758m	$\nu_{16}$	$\nu_{32}$	
756s	761mw							
702vw	710vw $\uparrow$	*	*	704m, P $\uparrow$	*			AA
679vs	683s $\uparrow$	*	685vs	677m, P $\uparrow$	*		$\nu_{33}$	
	679s	} 659vs	*	663s, D	657vs	$\nu_{40}$		
666vs	673vs							
654vs	660s	645vs	*	650vs, P	645vs	$\nu_{17}$		
	647vw	} $\uparrow$ *	643vs	640vs, P $\uparrow$	*		$\nu_{34}$	
642m	645mw							
629vw		629w	*	605vw, D $\uparrow$	*			AA
605w	611w $\uparrow$	*	*					
		602vvw	*					AA
492w	494w $\uparrow$	*	*	460w, P $\uparrow$	*		$\nu_{35}$	
460m	461w $\uparrow$	*	469s					
		447vw	*	443m, P	443s	$\nu_{41}, \nu_{18}$		
443w	443vvw	441vw						
421vvw		*	411w	403w, P $\uparrow$	*		$\nu_{36}$	
397vw	402vvw $\uparrow$	*	390m	376w, P $\uparrow$	*		$\nu_{37}$	
375vw	376vw $\uparrow$	*	*					
352vw	~340vvw?	341w	*	329mw, D	342vw	$\nu_{19}$		
327w	328vw	327mw	*	306w, P	327s	$\nu_{42}$		
317vw	304vvw	*	320w	282w, P? $\uparrow$	*		$\nu_{38}$	
283vw	284vw $\uparrow$	*	289m	272s, P	275s	$\nu_{20}$	$\nu_{39}$	
272vw	277vw	275w	*					
251vvw		266vw						
224vw	~226vvw?	222w	241w	201w, D	221vw	$\nu_{43}$	$\nu_{40}$	
		211m	224	190w, P $\uparrow$	212w	$\nu_{21}$	$\nu_{41}$	
203w		181mw	*	181w, P $\uparrow$	180mw	$\nu_{44}$		
~190?		*	199w	168m, P	*		$\nu_{42}$	
~180?		*	*	158w	*			AA?
169vw		157vw	*	~155?	*	$\nu_{22}$		
~152?		*	145w	123vw, D	116vw	$\nu_{45}$	$\nu_{43}$	
123vvw		109?	*					

Table I cont'd.

Infrared				Raman		Assignment <sup>b</sup>		
Liquid	Ar-matrix	Low. temp. crystal	High pressure crystal	Liquid	Low temp. crystal	GG	AG	AA
~108?		*	114w				$\nu_{44}$	
			95w				lat.	
88vw		*	~75w	83w, P?			$\nu_{45}$	
			72w		76w	lat.		
			~50w				lat.	
60vw			55w	50w	62m	$\nu_{23}$		
			40w		39mw			
			31w		21s			

<sup>a</sup> Many weak bands, particularly in the regions 4000—3100  $\text{cm}^{-1}$  and 2800—1500  $\text{cm}^{-1}$  were omitted.

<sup>b</sup> For the meaning of conformers GG, AG and AA see Figure 6.

<sup>c</sup> Abbreviations: s, strong; m, medium; w, weak; v, very; P, polarized; D, depolarized; asterisks (\*) denote vanishing bands; arrows ( $\uparrow$ ) denote bands enhanced at higher temperatures.

## DISCUSSION

## Conformers

Four staggered conformers of DBDMP are theoretically possible with symmetries and notation  $C_2$  (GG),  $C_1$  (AG),  $C_{2v}$  (AA) and  $C_s$  ( $GG_1$ ), as depicted in Figure 6. The conformer  $GG_1$  of  $C_s$  symmetry has one parallel 1,3-interaction between the C-Br bonds, leading to a decreased stability of the order of 15<sup>11</sup> to 35<sup>12</sup>  $\text{kJ mol}^{-1}$ , as calculated by molecular mechanics calculations. The  $GG_1$  conformer is accordingly of no interest when the conformational abundance in DBDMP is discussed, and attention will be focused upon the GG, AG and AA conformers as previously done for DCDMP.<sup>6</sup>

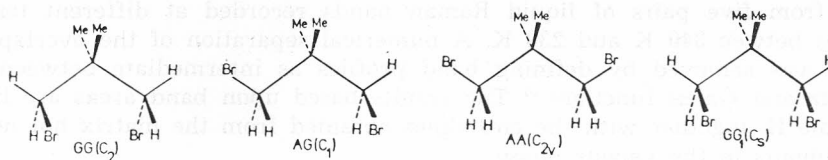


Figure 6. Possible conformers of DBDMP.

## Low Temperature Spectra

Deposition of DBDMP from vapour in either an infrared or a Raman cryostat led to an initially amorphous film. The spectra of this film were quite similar to those of the liquid. When the sample was annealed to approximately 180 K, it became crystalline and many bands vanished (Figures 1, 2, 5). Also when the liquid was slowly cooled in the Raman capillary,<sup>10</sup> the sample readily crystallized after an initial supercooling. The wave numbers of the vanishing bands are marked with asterisks in Table I. From the intensities of the disappearing bands in IR as well as in Raman, we feel

that the vanishing conformer(s) are present in less than 30% abundance at room temperature.

In the earlier studies of DBDMP and the corresponding chloro and iodo compounds dissolved in freon ( $\text{CBrF}_3$ ) by NMR spectroscopy<sup>11,13</sup> only the GG conformers were detected at the coalescence temperatures. Moreover, both of the two molecular mechanics calculations<sup>11,12</sup> list the relative stabilities in the order GG, AG, AA and GG<sub>1</sub> for DBDMP as well as for DCDMP although the relative values differ considerably between the two studies. From these results, from the close similarity of the persistent conformer spectra with those of DCDMP<sup>6</sup> and from the results of the normal coordinate analysis, it can be concluded without doubt that the GG conformer is present in the low temperature crystal. Given all these reasons we are also confident that the main conformer which disappears on crystallization is AG.

Since the complete IR spectrum of the AG conformer alone was recorded as a high pressure crystal (see below), we could detect some weak IR and Raman bands present in the liquid and in the amorphous phase which were present neither in the low temperature nor in the high pressure crystals. In the matrix isolated IR spectra these bands, although weak, showed large enhancements with higher nozzle temperatures, in accordance with a high  $\Delta H^\circ$  difference from the stable GG conformer. Undoubtedly, these bands are due to the AA conformer. The two most prominent bands at 704 and 605  $\text{cm}^{-1}$  attributed to the AA conformer (see Table I) fit quite well with the calculated frequencies of species  $a_1$  and  $b_2$  at 712 and 595  $\text{cm}^{-1}$ , respectively. In our preliminary paper<sup>9</sup>, submitted before the complete set of data was collected, we failed to recognize the existence of the third conformer (AA). Moreover, no third conformer was observed in our spectra of DCDMP<sup>6</sup> although ca. 7% of the AA conformer was suggested in the gaseous electron diffraction measurements at 333 K.<sup>1</sup> We now plan to record hot nozzle matrix spectra of DCDMP as well, in order to detect possible bands of the AA conformer in this molecule.

The enthalpy differences  $\Delta H^\circ$  between the three conformers were calculated from five pairs of liquid Raman bands recorded at different temperatures between 340 K and 230 K. A numerical separation of the overlapping bands was achieved by defining band profiles as intermediate between the Lorentz and Gauss functions.<sup>14</sup> The results based upon band areas are listed in Table II, together with the enthalpies obtained from the matrix hot nozzle experiments in the vapour phase.

### High Pressure Spectra

Application of approximately 15 kbars pressure in the diamond anvil cell was sufficient to produce an anisotropic crystal. Just as it had been earlier observed for DCDMP,<sup>6</sup> the conformer present at high pressure was not the one stable in the low temperature crystal. Rather, the high pressure crystal conformer was the major conformer which vanished when the low temperature crystal was formed. As it was mentioned earlier, we are confident that it is the AG conformer.

The variable temperature measurements of the liquid and of the vapours (observed in the matrices) reveal enthalpy differences of 4–5  $\text{kJ mol}^{-1}$



TABLE II  
 Thermodynamic Parameters Related to the Conformers of DBDMP

Conformers	Band pairs (cm <sup>-1</sup> )	Calculated $\Delta H^0$ (kJ mol <sup>-1</sup> ) from spectra		
		N <sub>2</sub> -matrix <sup>a</sup>	Ar-matrix <sup>a</sup>	Liquid <sup>b</sup>
AG/GG	1182/1177	4.51	4.02	—
	1080/1087	4.26	—	—
	904/ 921	4.22	3.52	5.93
	855/ 872	3.88	3.87	—
	683/ 673	4.89	4.44	5.32
	645/ 660	4.64	4.54	5.95
	460/ 443	—	—	5.02
	306/ 329	—	—	5.72
	283/ 273	3.96	4.37	—
$\Delta H^0$ (AG—GG)	[kJ mol <sup>-1</sup> ]	4.2 ± 0.4		5.6 ± 0.6
$K_{298}$ (AG—GG)		0.37		
$\Delta G^0_{298}$ (AG—GG)	[kJ mol <sup>-1</sup> ]	2.5		
$\Delta S^0$ (AG—GG)	[J K <sup>-1</sup> mol <sup>-1</sup> ]	5.8		
Conformers	Band pairs (cm <sup>-1</sup> )	Calculated $\Delta H^0$ (kJ mol <sup>-1</sup> ) from spectra		
		N <sub>2</sub> -matrix <sup>a</sup>	Ar-matrix <sup>a</sup>	Liquid <sup>b</sup>
AA/GG	1155/1177	5.95	6.66	—
	888/ 921	5.81	6.12	—
	611/ 660	7.14	7.27	—
	704/921	—	—	5.68
	704/673	—	—	6.77
	704/ 660	—	—	6.74
$\Delta H^0$ (AA—GG)	[kJ mol <sup>-1</sup> ]	6.5 ± 1.0		6.4 ± 0.8
$K_{298}$ (AA—GG)		0.036		
$\Delta G^0_{298}$ (AA—GG)	[kJ mol <sup>-1</sup> ]	8.2		
$\Delta S^0$ (AA—GG)	[J K <sup>-1</sup> mol <sup>-1</sup> ]	-5.8		

<sup>a</sup> Calculated from absorbance values.

<sup>b</sup> Calculated from band areas, see text.

between GG and AG (Table II). The same was true for DCDMP<sup>6</sup> although the exact values were not measured for this compound. The GG and AG conformers have statistical weights 2 and 4, respectively.

The  $\Delta G^0$  (AG—GG) values calculated in Table II at atmospheric pressure may change considerably with pressure. From the expression  $(\partial G/\partial p)_T = V$  we can derive  $\Delta G(P) - \Delta G(1) = \int_1^P \Delta V dP$  where  $\Delta G(P)$  and  $\Delta G(1)$  are the  $\Delta G$  (AG—GG) at pressure  $P$  and at 1 bar, respectively. Considering  $\Delta V$  (AG—GG) as constant in the pressure range we get:

$$\Delta G(P) \approx \Delta G(1) + (P - 1) \Delta V \approx \Delta G(1) + P \Delta V.$$

$\Delta G(P)$  will be different from  $\Delta G(1)$  depending upon  $\Delta V$ . Obviously, if  $\Delta V$  (AG—GG) =  $V_m$  (AG) -  $V_m$  (GG), in which  $V_m$ , the molar volume of each conformer, is negative,  $\Delta G(P)$  would be smaller than  $\Delta G(1)$  and the equilibrium displaced towards AG with increasing pressure. However, it is by no means obvious that the AG conformer should have a smaller volume

that the GG. It has been suggested<sup>15</sup> that the number of *gauche* interactions in each conformer should to a first level of approximation determine the relative molar volume of haloalkanes. However, the number of C...Br *gauche* interactions is the same (four) for GG and AG as well as for AA. It seems significant that the two dihaloneopentanes DBDMP and DCDMP<sup>6</sup> both crystallize in the AG conformer under pressure. The corresponding 1,3-dibromopropane<sup>16</sup> as well as 1,2,2,3-tetrachloropropane<sup>6</sup> with hydrogens and chlorines in the 2-positions, respectively, crystallize in the GG conformer in the low temperature as well as in the high pressure crystals.

Twice during the release of pressure, a phase was observed in the microscope which was almost certainly plastic, as judged from the appearance of »wavy lines«. However, this phase was apparently stable only in a quite small pressure range and we did not succeed in recording a spectrum. It is our experience from halogenated neopentanes<sup>5-7</sup> that the molecular motions within the plastic phase permit the presence of all conformers in equilibrium similar to the conditions in the vapour and liquid states.

### Matrix Spectra

Depositions of DBDMP both in the argon and nitrogen matrices (1 : 500 ratio) were made at nozzle temperatures of 300, 450 and 700 K. Implicit in the hot nozzle technique used for conformational analysis is the assumption that the thermodynamic equilibrium of the vapour at the nozzle temperature will be maintained<sup>17</sup> when the vapour mixture is trapped on the window at 14 K. It is our experience that for molecules with a high conformational barrier, such as the saturated halogenated hydrocarbons, the vapour conformational equilibrium is upheld in the matrix. On the other hand, for molecules with low conformational barriers such as ethylazide<sup>18</sup> the equilibrium is found to be quite different in the argon and in the nitrogen matrices. Moreover, if the barrier is very low (less than 5 kJ mol<sup>-1</sup>), a window temperature of 14 K is not sufficient to trap the unstable conformers. As recently observed for monohalogenated cyclobutanes<sup>19</sup>, the axial conformer was completely absent in the matrix spectra.

As seen from Figure 4, a number of IR bands of DBDMP in a nitrogen matrix change significantly in relative intensities from nozzle temperatures 300 to 700 K. The intensity variations with temperature were quite similar in the two matrices, and only the argon matrix data are included in Table I in which the enhanced bands are marked with vertical arrows. As it is apparent from Table I, the bands present in the high pressure crystal (AG) are enhanced with temperature; those present in the low temperature crystal (GG) diminish in relative intensities. In addition, the weak IR bands at 1155, 888, 710, 611 and 494 cm<sup>-1</sup> which are absent in both crystal spectra are enhanced with temperature and must belong to the AA conformer.

### Thermodynamic Functions

In order to calculate the enthalpy difference  $\Delta H^\circ$  between the conformers from band intensities at various temperatures, it is essential that the bands employed are »pure« (belong to one conformer only). Since DBDMP has 45 fundamentals for each conformer, fundamentals (or combination bands or

overtone) of one of the three conformers present can easily overlap with those of another conformer, leading to erroneous values. The conformational purity of the band pairs used in the calculations was therefore checked by the complete appearance/disappearance in the two crystal spectra and by the wavenumber separation obtained in the force constant calculations. As apparent from Table II, 13 band pairs (7 in the N<sub>2</sub> and 6 in the Ar matrices) were employed for GG/AG and 6 for the GG/AA calculations. Absorbance values, rather than band areas were used, and the results for each band pair treated by a least squares procedure. The  $\Delta H^\circ$  values between AG and GG calculated from the vapour phase (IR matrix) show slightly lower values than those obtained in the liquid (Raman).

From the average values of  $\Delta H^\circ$  (XX—GG) (in which XX = AG or AA) in Table II the equilibrium constants:

$$1) K(XX/GG) = [XX]/[GG] = (g(XX)/g(GG)) e^{-\Delta H^\circ(XX-GG)/RT}$$

were calculated. The Gibbs free energy functions  $\Delta G^\circ(XX-GG) = -RT \ln K(XX-GG)$  and the entropy  $\Delta S^\circ(XX-GG) = -[\Delta G^\circ(XX-GG) - \Delta H^\circ(XX-GG)]/T$  are obtained. From these equations we get  $\Delta S^\circ(XX-GG) = R \ln [g(XX)/g(GG)]$  in which  $g(XX)$  and  $g(GG)$  are the statistical weights of conformers XX and GG, respectively. Thus, if  $\Delta H^\circ(XX-GG)$  is temperature independent, the same is true for  $\Delta S^\circ(XX-GG)$ .

The total entropy difference  $\Delta S^\circ(XX-GG) = S^\circ(XX) - S^\circ(GG)$  between two spectroscopically distinguishable conformers in the vapour phase is:

$$2) \Delta S^\circ(XX-GG) = \Delta S^\circ_{\text{rot}}(XX-GG) + \Delta S^\circ_{\text{vib}}(XX-GG) + \Delta S^\circ_{\text{sym}}(XX-GG).$$

The terms  $\Delta S^\circ_{\text{rot}}$  and  $\Delta S^\circ_{\text{vib}}$  are the rotational and vibrational entropy differences, respectively, while  $\Delta S^\circ_{\text{sym}}$  include the changes in symmetry and optical activity. The rotational and vibrational entropy can be expressed as  $S_{\text{rot}} = R(3/2 + \ln Q_{\text{rot}})$  and  $S_{\text{vib}} = R[u/(e^u - 1) - \ln(1 - e^{-u})]$  in which  $Q_{\text{rot}}$  is the classical rotational partition function and  $u = hc\nu/kT$  where  $\nu$  are the wavenumbers of the normal vibrations (Table IV). The symmetry term of the entropy is  $S_{\text{sym}} = R \ln n/\sigma$  in which  $n$  and  $\sigma$  are defined in Table III. The  $S_{\text{rot}}$  and  $S_{\text{vib}}$  vary with temperature, but the calculations showed that they were nearly identical for the GG, AG and AA conformers. Therefore, their differences made negligible contributions to the entropy of Eq. 2, and the main part is connected with  $\Delta S^\circ_{\text{sym}}(XX-GG)$ .

Two of the argon matrices were annealed for 45 minutes at 35 K with no consistent change in the spectra, aside from minor differences ascribed to matrix effects. Even 12 hours annealing of the nitrogen matrix at 33 K led to no change in the conformational abundance. Thus, the barrier between the conformers must be at least 11 kJ mol<sup>-1</sup>, using the value 11.2 for log A<sup>20</sup> in the Arrhenius equation and assuming that a change as low as 5% would be detected.

### Normal Coordinate Analysis

Force fields for the various conformers of DBDMP were derived by transferring force constants employed in the studies of chloro-,<sup>5</sup> bromo-,<sup>21</sup> dichloro-,<sup>6</sup> trichloro-,<sup>7</sup> tetrachloro-<sup>8</sup> and tetrabromoneopentane.<sup>8</sup> We have used dimensionless internal stretching coordinates  $\Delta r/r_0$ , whereby it is possible to

TABLE III  
Principal Moments of Inertia, Symmetry Parameters and Entropy Terms for Conformers of DBDMP

Conformers:	GG	AG	AA
$I_A$ [amu Å <sup>2</sup> ] <sup>a</sup>	313.05	214.58	115.98
$I_B$ [amu Å <sup>2</sup> ]	754.46	1066.56	1378.67
$I_C$ [amu Å <sup>2</sup> ]	954.57	1167.69	1380.95
$g$ (XX) <sup>b</sup>	2	4	1
$n$	2	2	1
$\sigma_c$	2	1	2
$\pi\sigma_i$	9	9	9
$\sigma = \sigma_c \cdot \pi\sigma_i$	18	9	18
$Q_{rot}$ (298K)	$1.160 \times 10^6$	$1.262 \times 10^6$	$1.148 \times 10^6$
$Q_{rot}$ (700K)	$4.171 \times 10^6$	$4.542 \times 10^6$	$4.128 \times 10^6$
$S_{rot}^0$ (298K) <sup>c</sup>	128.56	129.27	128.48
$S_{rot}^0$ (700K)	139.21	139.91	139.12
$S_{vib}^0$ (298K)	100.44	99.58	100.41
$S_{vib}^0$ (700K)	241.51	240.69	241.50
$S_{sym}^0$	-18.27	-12.50	-24.03
$\Delta S_{298}^0$ (XX—GG)	—	5.62	-5.87
$\Delta S_{700}^0$ (XX—GG)	—	5.65	-5.86

<sup>a</sup> Principal moment of inertia; assuming C—H, 1.093Å; C—C, 1.54Å; C—Br, 1.94Å and all angles tetrahedral.

<sup>b</sup>  $g$  (XX) — statistical weight of conformers (XX = GG, AG, AA).

$n$  — number of distinguishable conformers.

$\sigma_c$  — symmetry number refers to the symmetry of the entire molecule.

$\pi\sigma_i$  — product of symmetry numbers of those parts of the molecule which can rotate around its single bonds.

<sup>c</sup> All entropy terms are in [J K<sup>-1</sup> mol<sup>-1</sup>].

reduce<sup>22</sup> considerably the number of different force constants in a series of halogen substituents. The procedure has been described<sup>7,22</sup> earlier. A 41 parameter force field was derived by a least squares treatment of *ca.* 280 observed frequencies below 1500 cm<sup>-1</sup>, taken from the various conformers of the halogenated neopentanes.<sup>5-8,21</sup> Our results for the three important conformers GG, AG and AA are listed in Table IV together with the wave-numbers of the observed vibrational bands assigned as fundamentals.

### Spectral Interpretation

The observed vibrational bands assigned as fundamentals for the GG, AG and AA conformers are listed in Table IV, together with the results of the force constant calculations. Since spectra of the isolated GG and AG conformers were recorded in the low temperature and in the high pressure crystals, respectively, these interpretations should be quite reliable. A large number of bands were present in both crystals, revealing coinciding GG and AG fundamentals. Frequently, this was supported by the matrix spectra, showing separate peaks for each conformer in one or both matrices. To keep the size of Table I within reasonable limits, the nitrogen matrix data were omitted, as were certain weak peaks in the argon matrix spectra.

With low symmetry of the two most abundant conformers GG (two-fold axis) and AG (no symmetry), the Raman polarization data had limited significance. However, all the polarized bands were attributed either to  $a$ -modes

TABLE IV

Observed and Calculated Fundamental Frequencies for the Conformers of DBDMP

$\nu$	GG			AG		AA		
	Obs. <sup>a</sup>	Calc.	PED <sup>b</sup>	Obs. <sup>c</sup>	Calc.	Obs.	Calc.	
1	3006	3009	a	CH <sub>2</sub> as(99)	3031	3008	3007	b <sub>1</sub>
24	3006	3007	b	CH <sub>2</sub> as(99)	3019	3007	3007	a <sub>2</sub>
2	2966	2967	a	CH <sub>2</sub> ss(96)	2984	2967	2966	b <sub>2</sub>
25	2966	2966	b	CH <sub>2</sub> ss(96)	2978	2966	2966	a <sub>1</sub>
3	2966	2963	a	CH <sub>3</sub> as(97)	2966	2964	2963	a <sub>1</sub>
26	2966	2961	b	CH <sub>3</sub> as(99)	2966	2962	2963	b <sub>2</sub>
4	2941	2961	a	CH <sub>3</sub> as(96)	2941	2961	2961	a <sub>2</sub>
27	2931	2960	b	CH <sub>3</sub> as(96)	2928	2960	2960	b <sub>1</sub>
5	2894	2883	a	CH <sub>3</sub> ss(99)	2896	2884	2884	a <sub>1</sub>
28	2872	2883	b	CH <sub>3</sub> ss(99)	2877	2883	2883	b <sub>1</sub>
29	1470	1464	b	CH <sub>3</sub> aδ(84), CH <sub>3</sub> r(10)	1471	1468	1475	a <sub>1</sub>
6	1463	1461	a	CH <sub>3</sub> aδ(85), CH <sub>3</sub> r(9)	1461	1463	1463	b <sub>2</sub>
30	1460	1458	b	CH <sub>3</sub> aδ(87), CH <sub>3</sub> r(8)	1456	1457	1456	b <sub>1</sub>
7	1443	1454	a	CH <sub>3</sub> aδ(91), CH <sub>3</sub> r(7)	1446	1453	1452	a <sub>2</sub>
8	1428	1412	a	CH <sub>2</sub> δ(66), BrCHδ(27)	1431	1407	1407	b <sub>2</sub>
31	1423	1410	b	CH <sub>2</sub> δ(66), BrCHδ(28)	1420	1406	1407	a <sub>1</sub>
9	1384	1380	a	CH <sub>3</sub> sδ(97), CCs(5)	1380	1386	1389	a <sub>1</sub>
32	1366	1377	b	CH <sub>3</sub> sδ(99), CCs(4)	1367	1375	1373	b <sub>1</sub>
33	1286	1296	b	CCs(39), BrCHδ(19)	1291	1297	1297	b <sub>1</sub>
10	1270	1292	a	CCs(43), CH <sub>2</sub> tw(18)	1275	1282	1289	b <sub>2</sub>
34	1257	1267	b	CH <sub>2</sub> w(24), CH <sub>2</sub> r(19)	1260	1281	1270	a <sub>1</sub>
11	1223	1230	a	CH <sub>2</sub> w(40), BrCHδ(39)	1220	1222	1208	a <sub>1</sub>
35	1172	1181	b	CCs(38), BrCHδ(23)	1185	1192	1191	b <sub>2</sub>
12	1126	1111	a	BrCHδ(32), CH <sub>2</sub> tw(28)	1123	1120	1155*	a <sub>2</sub>
36	1079	1095	b	BrCHδ(36), CH <sub>3</sub> r(21)	1079	1080	1066	b <sub>1</sub>
13	1012	1018	a	CH <sub>3</sub> r(85), CH <sub>3</sub> aδ(5)	1018	1019	1019	a <sub>2</sub>
37	947	952	b	CH <sub>3</sub> r(57), CCs(36)	983	953	953	a <sub>1</sub>
14	958	947	a	CCs(35), CH <sub>3</sub> r(31)	951	949	952	b <sub>1</sub>
38	917	912	b	CCs(52), CH <sub>3</sub> r(39)	910	914	888*	b <sub>2</sub>
15	866	860	a	CCs(33), CH <sub>3</sub> r(26)	861	854	848	a <sub>2</sub>
39	830	838	b	CH <sub>2</sub> r(36), BrCHδ(34)	853	842	843	b <sub>1</sub>
16	756	760	a	CCs(81), CBrs(7)	763	758	757	a <sub>1</sub>
40	666	674	b	CBrs(72), CCCδ(22)	685	679	710*	a <sub>1</sub>
17	654	650	a	CBrs(74), CCBrd(19)	643	644	611*	b <sub>2</sub>
18	443	445	a	CCCδ(67), CBrs(6)	469	454	494*	b <sub>2</sub>
41	443	443	b	CCCδ(67), CBrs(7)	411	402	402	b <sub>1</sub>
19	352	340	a	CCCδ(92), CH <sub>2</sub> Brτ(9)	390	382	377	a <sub>1</sub>
42	327	323	b	CCCδ(60), CBrs(40)	320	308	342	a <sub>2</sub>
20	272	263	a	CCCδ(47), CBrs(24)	289	274	268	b <sub>2</sub>
43	224	246	b	CH <sub>3</sub> τ(91), Br..Hs(5)	241	255	238	a <sub>2</sub>
21	211	238	a	CH <sub>3</sub> τ(78), CCCδ(10)	224	239	214	b <sub>2</sub>
44	203	188	b	CCBrδ(42), Br..Hs(25)	199	176	181?	a <sub>1</sub>
22	169	167	a	CCBrδ(44), Br..Hs(24)	145	155	137	a <sub>2</sub>
45	123	138	b	CH <sub>2</sub> Brτ(70), BrCHδ(9)	114	105	108	a <sub>1</sub>
23	60	47	a	CH <sub>2</sub> Brτ(73), BrCHδ(12)	~75	73	71	b <sub>1</sub>

<sup>a</sup> IR liquid phase values.<sup>b</sup> Potential energy distribution defined as  $X_{ik} = 100F_{ik}L^2/\lambda_{ik}$ ; a, asymmetric; s, symmetric; s, stretch; δ, deformation; r, rock.; w, wag.; tw, twist.; τ, torsion; Br. Hs, non bonded stretch interaction.<sup>c</sup> IR high pressure crystal values.

\* Values from Ar-matrix.

of GG, or to AG or overlapping GG and AG fundamentals. An exception is the polarized band at  $704\text{ cm}^{-1}$  attributed to the  $a_1$  mode  $\nu_{11}$  of the AA conformer, associated with C—Br stretch.

The two torsional modes of the  $\text{CH}_2\text{Br}$  groups were calculated to lie above and below  $100\text{ cm}^{-1}$  for each of the conformers. They were tentatively assigned to weak IR and Raman bands in the low frequency region (Tables I and IV) and correspond to similar data recorded for 1,3-dibromopropane.<sup>23</sup>

The agreement between the observed and calculated fundamentals is satisfactory for all the conformers. It should be stressed that the force field was transferred from the work on other neopentanes and was not at all adjusted to the present spectra. Some of the weaker bands in Table I which were not assigned as fundamentals are interpreted as combination bands or overtones. Certain low frequency bands observed in the crystal spectra are undoubtedly lattice modes.

*Acknowledgement.* The authors are grateful to A. Horn for drawing the figures and to G. Isaksen for purifying the sample. A. G. received a post-doctorate fellowship from NTNF. D.L.P. received support from the Norwegian Marshall Fund and from NAVF.

## REFERENCES

1. R. Stølevik, *Acta Chem. Scand.* **28A** (1974) 299, 327, 455.
2. J. G. Aston and G. H. Messerley, *J. Amer. Chem. Soc.* **58** (1936) 2354.
3. J. C. Trowbridge and E. F. Westrum Jr., *J. Phys. Chem.* **68** (1964) 255.
4. H. L. Clever, W. K. Wong, and E. F. Westrum Jr., *J. Phys. Chem.* **69** (1965) 1209.
5. P. Klaeboe, C. J. Nielsen, and D. L. Powell, *Spectrochim. Acta* **41A** (1985) 1315.
6. D. L. Powell, P. Klaeboe, K. Saebø, and G. A. Crowder, *J. Mol. Struct.* **98** (1983) 55.
7. K. Martinsen, D. L. Powell, C. J. Nielsen, and P. Klaeboe, *J. Raman Spectrosc.* **17** (1986) 437.
8. P. Klaeboe, B. Klewe, K. Martinsen, C. J. Nielsen, D. L. Powell, and D. J. Stubbles, *J. Mol. Struct.* **140** (1986) 1.
9. A. Gatial, M. Horn, P. Klaeboe, C. J. Nielsen, and D. L. Powell, *J. Mol. Struct.* (1988) in press.
10. F. A. Miller and B. M. Harney, *Appl. Spectrosc.* **2** (1970) 291.
11. M. R. Whalon, G. L. Grady, P. McGoff, R. P. Domingue, and C. H. Bushweller, *Tetrahedron Lett.* **23** (1982) 5247.
12. R. Stølevik and P. Bakken, *J. Mol. Struct.* **144** (1986) 301.
13. C. H. Bushweller, M. R. Whalon, S. H. Fleischman, C. D. Rithner, and J. S. Sturges, *J. Amer. Chem. Soc.* **101** (1979) 7073.
14. M. Horák and A. Vitek, *Interpretation and Processing of Vibrational Spectra*, John Wiley, Chichester, 1978, page 44.
15. F. Shahidi, P. G. Farrell, and J. T. Edward, *J. Phys. Chem.* **83** (1979) 419.
16. J. Thorbjørnsrud, O. H. Ellestad, P. Klaeboe, and T. Torgrimsen, *J. Mol. Struct.* **15** (1973) 61.
17. Hs. H. Günthard, *J. Mol. Struct.* **80** (1982) 87.
18. C. J. Nielsen, K. Kosa, H. Priebe, and C. E. Sjögren, *Spectrochim. Acta* **44A** (1988) in press.
19. D. L. Powell, A. Gatial, P. Klaeboe, C. J. Nielsen, and A. J. Kondow, *J. Mol. Struct.* (1988) in press.
20. R. Pong, T. D. Goldfarb, and A. Krantz, *Bunsenges. Phys. Chem.* **82** (1978) 9.
21. G. A. Crowder, C. Harper, and H.-R. Jalilian, *J. Mol. Struct.* **49** (1978) 403.

22. T. Woldbaek, C. J. Nielsen, and P. Klaeboe, *J. Mol. Struct.* **66** (1980) 31.
23. J. E. Gustavsen, P. Klaeboe, and R. Stølevik, *J. Mol. Struct.* **50** (1978) 285.

### SAŽETAK

#### **Konformacije i vibracijski spektri, uključujući matičnu izolaciju, 1,3-dibromo-2,2-dimetilpropana**

*A. Gatial, P. Klaeboe, C. J. Nielsen i D. L. Powell*

Snimljeni su infracrveni spektri 1,3-dibromo-2,2-dimetilpropana u tekućini i dva kristalna stanja pri niskoj temperaturi i pri visokom tlaku. Dodatni infracrveni spektri ovoga spoja, izoliranog u matricama argona i dušika pri 14 K, dobiveni su korištenjem temperatura sapnice od 300, 400 i 700 K. Ramanovi spektri, uključujući polarizacijska mjerenja, snimljeni su pri različitim temperaturama između 340 i 230 K. Kristali su dobiveni smrzavanjem tekućine i smrzavanjem šokom pri 85 K uz napuštanje.

Konformer *GG* i *AG* prisutni su u kristalima pri niskoj temperaturi, odnosno visokom tlaku, dok je razlika u entalpiji 5,6 (tekućina) i 4,2 kJ mol<sup>-1</sup> (para), pri čemu je *GG* stabilniji. U spektrima tekućine i matrici detektiran je dodatni konformer *AA*, koji je nestabilniji od konformera *GG* za približno 6,4 kJ mol<sup>-1</sup> u tekućini, odnosno 6,5 kJ mol<sup>-1</sup> u pari. Prikazana je vibracijska asignacija *GG* i *AG* spektara, podržana analizom normalnih koordinata.